Beach growth driven by intertidal sandbar welding

Cohn, Nicholas; Ruggiero, Peter; de Vries, Sierd; García-Medina, Gabriel

Publication date
2017

Document Version
Final published version

Published in
Proceedings of Coastal Dynamics 2017

Citation (APA)
Cohn, N., Ruggiero, P., de Vries, S., & García-Medina, G. (2017). Beach growth driven by intertidal sandbar welding. In T. Aagaard, R. Deigaard, & D. Fuhrman (Eds.), *Proceedings of Coastal Dynamics 2017: Helsingør, Denmark* (pp. 1059-1069). Article Paper No. 199

Paper No. 199 in Proceedings of Coastal Dynamics 2017, 12-16 June 2017 Helsingør, Denmark
ed. Troels Aagaard, Rolf Deigaard, David Fuhrman

BEACH GROWTH DRIVEN BY INTERTIDAL SANDBAR WELDING

Nicholas Cohn[1], Peter Ruggiero[1], Sierd de Vries[2] and Gabriel García-Medina[3]

Abstract

Seasonal variability in wave conditions drive corresponding cycles of erosion and accretion along sandy beaches. Despite the fact that these oscillations are well documented at numerous sites throughout the world, the physical processes driving beach recovery remain poorly understood. Using field data from a low sloping, dissipative beach in the U.S. Pacific Northwest we show that the onshore migration of intertidal sandbars contributes to beach growth in a rapidly prograding system. Over a six week period two intertidal sandbars are shown to migrate onshore resulting in the generation of a low relief berm and local beach width increases of up to 20 m. Although significant alongshore variability of intertidal morphological change was observed, a 2.5 km stretch of coast is shown to experience beach growth as a result of intertidal bar welding.

Key words: beach recovery, intertidal sandbars, sediment transport, morphodynamics, shoreline change

1. Introduction

During periods of calm wave conditions, nonlinear waves generally drive net onshore transport, with rates largely dependent on the details of the hydrodynamics, sediment characteristics, and beach slope. Onshore sediment transport in the surf zone is primarily driven by wave orbital velocity skewness, wave acceleration asymmetry, and boundary layer streaming (e.g., Aagaard et al., 2012; Elgar et al., 2001; Thornton et al., 1996), whereas undertow induces offshore transport. Although onshore-directed processes operate on the time scale of individual waves, it is the aggregation of small fluxes over large length- and time-scales that drives net onshore transport landward across the surf zone to the intertidal zone.

The intertidal zone is particularly complex as it is influenced by wave dissipation, swash processes, spatially and temporally variable grain size distributions, groundwater dynamics, and temporal modulation in the mean water surface by tides and other processes. As a result of numerous morphodynamic feedback mechanisms, intertidal sandbars are relatively ubiquitous features (Masselink et al., 2006). Under fair weather conditions these features migrate landward as a combined result of nonlinear wave and swash processes. When the tidal stage is close to the bar crest elevation, individual swash excursions overtop the bar with sediment entrained from the bar driving a net landward flux of sediment (Wijnberg and Kroon, 2002). However, Kroon and Masselink (2002) found that surf zone processes play a primary role in onshore intertidal bar migration over these swash processes. During low energy conditions breaking waves and bores advancing over sandbars in shallow water erode sediment from the seaward bar slope and deposit sediment on the slip-face, resulting in a net onshore migration of the feature (Sunamura and Takeda, 1984). As the spring-neap cycle modulates the residence time of wave breaking over the bar crest, temporal variation in tides has been recognized as another important driver of intertidal bar evolution (Kroon and Masselink, 2002). Driven by these combined wave and tidal processes, intertidal bars can migrate landward at rates of ~1 (Cohn et al., 2015) to over 10 m/day (Masselink et al., 2006). This landward migration provides a new sediment supply to the intertidal zone, which is thought to be the primary source area for aeolian sediment transport on the beach (e.g., de Vries et al., 2014). In the case that an intertidal sandbar

[1] College of Earth, Ocean, and Atmospheric Sciences, Oregon State University, cohnn@geo.oregonstate.edu; pruggier@coas.oregonstate.edu
[2] Faculty of Civil Engineering and Geosciences, Delft University of Technology, The Netherlands, sierd.devries@tudelft.nl
[3] College of Engineering, Oregon State University, USA, ggarcia@coas.oregonstate.edu

welds to the shoreline, the dry beach width increases as well, correspondingly increasing the beach fetch length. Consequently, bar welding events are thought to be an important source of sediment for dune growth (Houser et al., 2009).

While intertidal sandbars are fairly ubiquitous features in calm conditions, their formation and evolution remain poorly understood. To explore the role of bar migration and welding on nearshore-beach-dune exchanges, detailed morphologic and hydrodynamic measurements of sandbar evolution were made during the Sandbar Aeolian Dune Exchange Experiment (SEDEX^2) over a 6 week period in summer 2016 in Oysterville, WA, USA. Using detailed morphology and hydrodynamic data from the inner surf zone, intertidal, and beach, we explore the spatio-temporal trends in onshore bar migration that contribute to beach growth observed during the experiment. Here we provide an overview of the study site (Section 2) and introduce some of the measurements made during SEDEX^2 (Section 3). In Section 4 we document the morphological change and processes associated with the observed sandbar welding while in Section 5 we provide a discussion of key findings and initial conclusions.

2. Geographic Setting

The U.S. Pacific Northwest coast is a modally dissipative, mesotidal system with a wide range of morphologies including dune, bluff, and headland backed beaches. This high energy region has a strongly seasonal wave climate with average wave heights of about 2 m and 3.5 m in the summer and winter, respectively (Allan and Komar, 2002). Resulting in part from an abundant sediment supply from the Columbia River, the Long Beach Peninsula experiences a modern shoreline growth of over 4 m/yr (Ruggiero et al., 2005, 2016). A coastal monitoring program focused on the Columbia River littoral cell has documented the seasonal- to decadal-scale evolution of the active coastal profile from approximately -12 m (MLLW) to landward of the active foredune. The nearshore zone in the Oysterville section of Long Beach Peninsula (Figure 1) is characterized by two to four subtidal sandbars, a low sloping beach ($\tan\beta \sim 0.025$), and densely vegetated dunes which are accumulating sediment at a rate of amount 10 m^3/m/yr (Ruggiero et al., 2016). In the summer there are also typically low amplitude (< 1 m), slip-face intertidal sandbars which are notably absent in winter. Although the system exhibits a net interannual shoreline progradation, the seasonal wave climate drives corresponding oscillations in the shoreline position. The most eroded state occurs in late spring (ca. March/April) and the most prograded in fall (ca. September/October). Although these trends in coastal change are well documented (Ruggiero et al., 2005) via extensive quarterly surveying efforts, corresponding process measurements had not been made detailing the physical mechanisms driving beach and dune growth in these dynamic, dissipative systems until the experiment described in this paper.

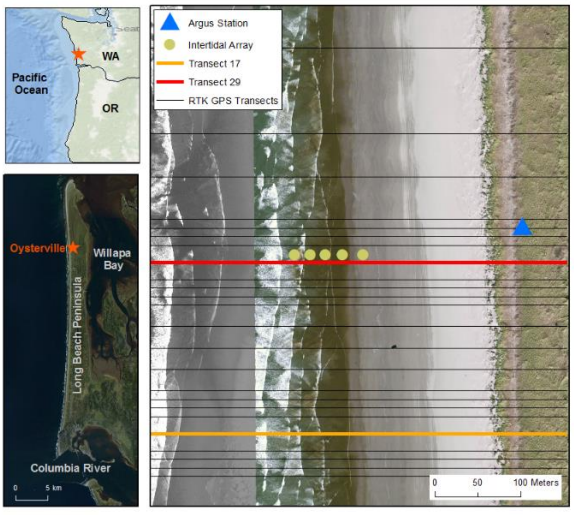

Figure 1. Map of study area in Oysterville, WA at regional (upper left panel), littoral cell (lower left panel), and local (right panel) scales. Morphology and hydrodynamic measurement locations collected on the beach during SEDEX^2 are shown on the local panel.

3. Field Measurements

3.1 Overview of Field Experiment

The primary aim of SEDEX^2 was to measure the evolution of intertidal sandbars and the hydrodynamic processes driving changes to intertidal sandbars along a rapidly prograding stretch of coast. The 6 week long measurement period, 1 August 2016 through 9 September 2016, was chosen based on (1) the characteristically low wave energy conditions during late summer and (2) just prior to when the maximum seasonal shoreline position generally occurs in the Pacific Northwest (Barnard et al., 2017; Cohn et al., 2015). Coastal morphological change was measured on time scales as short as daily to adequately detail intertidal bar dynamics. Synoptic measurements of waves, currents, water levels, runup, suspended subaqueous sediment transport, aeolian sediment transport, groundwater levels, moisture dynamics, meteorological conditions, and vegetation characteristics were also collected during SEDEX^2 in order to compile a comprehensive dataset for investigating processes related to beach and dune growth.

3.2 Environmental Conditions

Hydrodynamic measurements during SEDEX^2 spanned almost three full spring-neap cycles. As measured from a Nortek Acoustic Wave and Current Profiler (AWAC) deployed at -8.5 m MLLW (-8.8 m NAVD88) offshore of the study area, sea-swell conditions were prevalent during the experiment with significant wave heights between 0.5 and 2 m (Figure 2). Although wave periods were generally between 6 and 9 s, peak wave periods reached 20 s during the experiment. Two meteorological stations, a Dyacon MS-140 and a NexSens WS-100 were deployed on the primary and secondary dunes, respectively, to provide information on the local wind climate. The mean wind speed during the experiment was 3 m/s (Figure 2) with the predominant wind direction from the SSW.

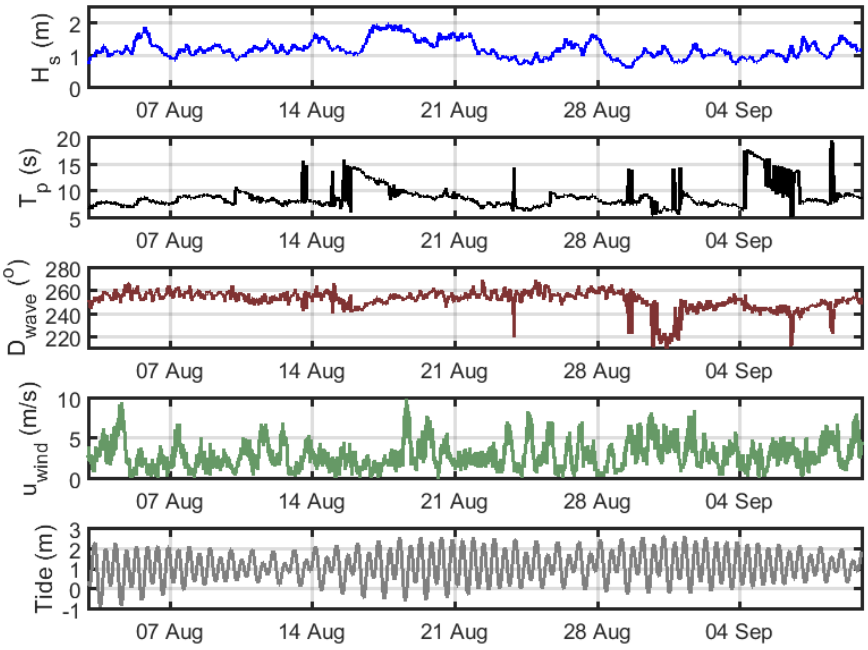

Figure 2. Environmental conditions during SEDEX^2. Tide values in NAVD88.

3.3 Morphology Measurements

To measure short-term coastal change, topography in the intertidal zone and backshore were measured using backpack based real-time kinematic (RTK) GPS along multiple cross-shore transects. Twenty cross-

shore transects spanning 1 km in the alongshore were measured at daily intervals with an additional twenty transects measured nominally at weekly time intervals over a larger spatial span (2.5 km). These transects were completed around low tide during each survey to maximize coverage of the intertidal zone. Additionally, a terrestrial lidar scanner was regularly used throughout the experiment to measure high resolution data over portions of the intertidal zone and backshore (de Vries et al., this volume). Although most measurements for SEDEX^2 were limited to a 6 week period, RTK topographic measurements were also completed in spring 2016, fall 2016, and winter 2017 to provide context into the sub-seasonal morphology change at the site.

Nearshore bathymetric measurements of the inner and outer surf zone were collected at approximately bi-weekly intervals using the Coastal Profiling System (Ruggiero et al., 2005, Di Leonardo and Ruggiero, 2015) at the offshore portion of some of the cross-shore topographic survey lines. The bathymetric surveys were timed at high tide to provide overlap with the onshore based measurements. A three day long comprehensive multi-beam survey was also completed at the beginning of the experiment to provide comprehensive spatial depiction of the subtidal morphology, providing detailed morphology data as shallow as -1 m NAVD88.

To provide additional information on the intertidal and backshore morphology, an Argus camera system (Holman and Stanley, 2007) was mounted on an 8 m mast installed on top of the foredune crest (Figure 1). At spring low tide this temporary Argus station captured information along a 500 m alongshore extent of coast. The Argus platform enabled snapshots, variances images, time exposures, and a range of other products relevant for extracting both qualitative and quantitative morphologic properties.

3.4 Inner Surf Zone Hydrodynamic Measurements

In order to investigate the hydrodynamic processes influencing the evolution of the intertidal morphology, a series of instruments were installed in a cross-shore array in the intertidal zone along Transect 29 (Figure 1). At any time up to three 64 Hz Nortek Vectors, two 2 Hz RBR Solo pressure sensors, and four 16 Hz RBR Solo pressure sensors were deployed. Collectively, these instruments provide insight into the cross-shore transformations of inner surf zone waves, including infragravity waves, wave orbital velocities, and mean currents. The Argus mast also collected time stacks for digitizing runup each hour during daylight. Additionally, GPS-equipped drifters were deployed in the inner surf zone four times during SEDEX^2 to measure near-surface current velocities and circulation patterns. While all of these hydrodynamic measurements are important for understanding intertidal sandbar dynamics, in this paper we report only on a subset of the pressure sensor output to explore spatio-temporal variability in wave and water level properties and the resulting implications on onshore intertidal bar migration.

4. Results

4.1 Observed Intertidal Morphology Change

4.1.1. Cross-shore behavior

During SEDEX^2, the coastal zone at Oysterville was characterized by 4 sandbars, 2 subtidal and 2 intertidal. Repeat bathymetric and topographic measurements document onshore migration of each of these bar features (Figure 3a). The slip-face of the outermost subtidal bar (SB1) migrated onshore about 15 m during the experiment. During the experiment there was notable deflation of the SB1 stoss slope of up to 0.2 m while the landward SB1 trough aggraded by about 0.5 m. Despite large net landward fluxes of sediment from SB1, the bar crest elevation did not change during the experiment period. Conversely, the SB2 bar crest aggraded by over 0.5 over this timeframe. At transect 17 (Figure 3a), which is located 200 m south of the intertidal instrument array, data gaps exist in water depths less than 2 m for certain periods of time, but data from nearby transects (not shown) indicates that SB2 migrated onshore by about 60 m total during the experiment.

A bar present at the base of the intertidal zone (IB3), which was partially exposed during spring low tides, exhibited significant temporal variability during the experiment. The IB3 bar height (crest to landward trough) varied between 0.3 and 1.2 m and migrated onshore about 30 m. Migration of the bar

crest was episodic in time, with mean and maximum bar migration rates of 1.2 and 12.3 m/day, respectively (Figure 4). The day with the maximum rate of bar migration of IB3 occurred during a day with average wave conditions and a spring high tide.

The landward most intertidal sandbar (IB4) began as a low relief feature at the start of the experiment (< 0.2 m), but its crest to trough height increased as it migrated landward with time. The volume of IB4, measured as the total volume between the landward and seaward bar troughs, also increased during the summer and resulted in a net increase in volume within the intertidal zone (Figure 4). By the end of the experiment IB4 migrated onshore over 100 m at which time the bar crest was located just below the mean high water (MHW) tidal datum (2.1 m NAVD88; Figure 4). As IB4 approaches MHW, sediment was shed off of IB4 and transported landward via swash processes resulting in the generation of a berm at the upper limit of the swash zone. The berm aggraded locally by up to 0.5 m and resulted in progradation of the dry beach by about 20 m between the start and end of the experiment.

The morphology data shows that there are complex spatial gradients in sediment transport (Figure 3b). As each of the four sandbars migrated onshore there was deflation on the stoss slope and accretion within the trough (Figure 3b). Integrating these measured vertical changes, there is a net onshore cumulative sediment flux from the shoreface to the base of the intertidal zone ($Q_x > 0$ for $x > 450$ m) (Figure 3c). However, the sediment budget is not closed when considering the entire coastal profile ($Q_x \neq 0$ at $x = 0$). Factoring in vertical uncertainty of RTK GPS can close the sediment budget if the errors are assumed to be biased and not random. Alternately, as Q_x only represents the cross-shore sediment flux then gradients in longshore processes potentially contribute to sediment export from the coastal profile. The cross-shore location where Q_x becomes negative coincides with the trough of IB3 where longshore currents were strong and showed spatially complex patterns (not shown), as measured by both drifter and Argus data during the experiment. This further supports the important role longshore processes have on the local bar dynamics and sediment transport pathways.

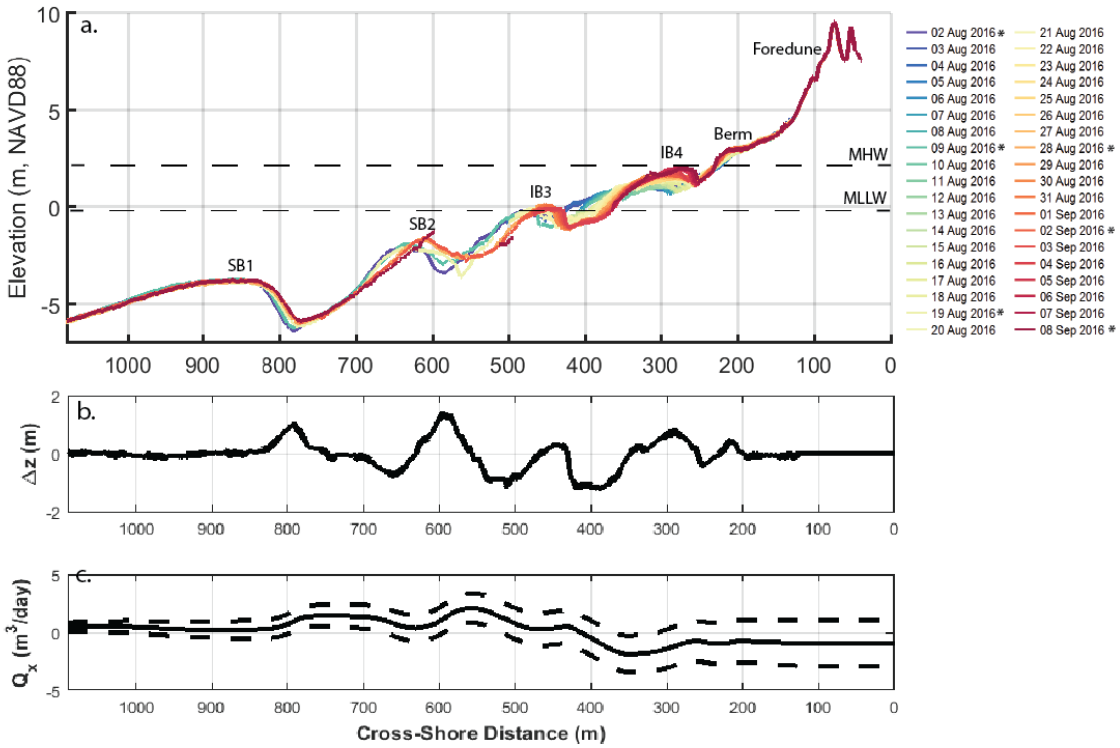

Figure 3. (a) Evolution of subtidal sandbar 1 (SB1), subtidal sandbar 2 (SB2), intertidal sandbar 3 (IB3), and intertidal sandbar 4 (IB4) along Transect 17 (* indicates bathymetric survey date), (b) change in elevation between 2 August 2016 and 2 September 2016, (c) cumulative cross-shore sediment flux integrated starting from offshore SB1 for the same survey dates. Dotted lines in (c) indicate uncertainty in Q_x based on vertical measurement accuracy.

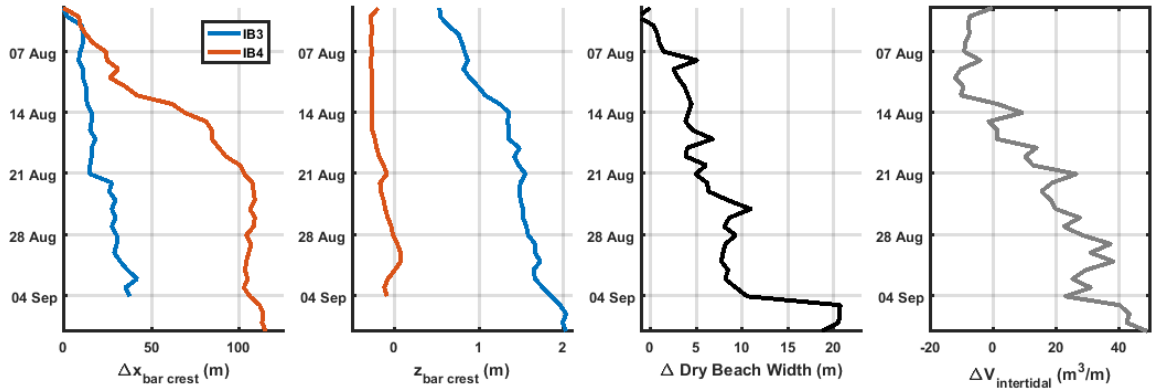

Figure 4. Evolution of IB3 and IB4 bar crest locations (left panel) and bar crest elevations (left middle panel), changes to dry beach width (right middle panel), and intertidal zone volume change (right panel) during SEDEX^2 at Transect 17

4.1.2. Alongshore variability in morphology change

Just prior to the start of the field experiment a high wave event with significant wave heights over 3 m occurring during spring tide on 30 July 2016 dampened the morphology that was present at the site (not shown). Both IB3 and IB4, which were present before this high energy event, either retreated seaward and/or were reduced in height. As part of this reorganization of the intertidal zone, spatially complex drainage patterns were present in the swash zone at the start of the experiment as shown by an Argus time exposure taken at mid-tide on 6 August 2016 in Figure 6. This resulted in significant alongshore variability in the cross-shore location and height of IB4 early in the experiment. However, SB1, SB2, and IB3 exhibited relative alongshore uniformity based on Argus (Figure 5) and bathymetric measurements taken at the start of the experiment.

Over the first few weeks of SEDEX^2, IB4 increased in height and migrated onshore throughout the study site resulting in a more organized bar trough between IB4 and the berm. While IB4 became more alongshore uniform, a rip channel developed in IB3 as can be seen in the Argus time exposure from 7 September 2016 in Figure 5. The local decrease in elevation at IB3 at this rip channel (0 m < Y < 50 m, X ≈ 380) is also shown in elevation difference plot between 2 August 2016 and 2 September 2016 within the Argus field of view. As this channel dissected the bar, increased wave energy influenced the intertidal zone directly landward, resulting in a decreased IB4 height at Transect 29 and adjacent transect lines.

A low amplitude berm developed across the entirety of the 2.5 km long study site. Using an approximate berm mid-point of 2.5 m NAVD88, we show that there was average (maximum) progradation of the dry beach of 10 m (20.6 m) during the experiment (Figure 6). Associated with the development of this feature, between 4.6 and 11.4 m^3/m of sediment accumulated between the 2 m and 3 m contours during SEDEX^2. As a result of the growth and migration of intertidal sandbars during the experiment and the fact that the bars had not fully welded by the end of the 6 week observational period, net volumetric changes within the lower intertidal zone (1 to 2 m) are generally higher than above MHW (2 m to 3 m) (Figure 6). Between the 1 m and 2 m contours there was an addition of up to 37.4 m^3/m of sediment. The data shows that although onshore intertidal sandbar migration occurs throughout the entire study site, complex feedback mechanisms result in significant alongshore variability in beach growth rates. Some of this variability appears related to the geometry of the sandbars and outlet channels draining bar troughs – although other complex internal dynamics likely also play a role.

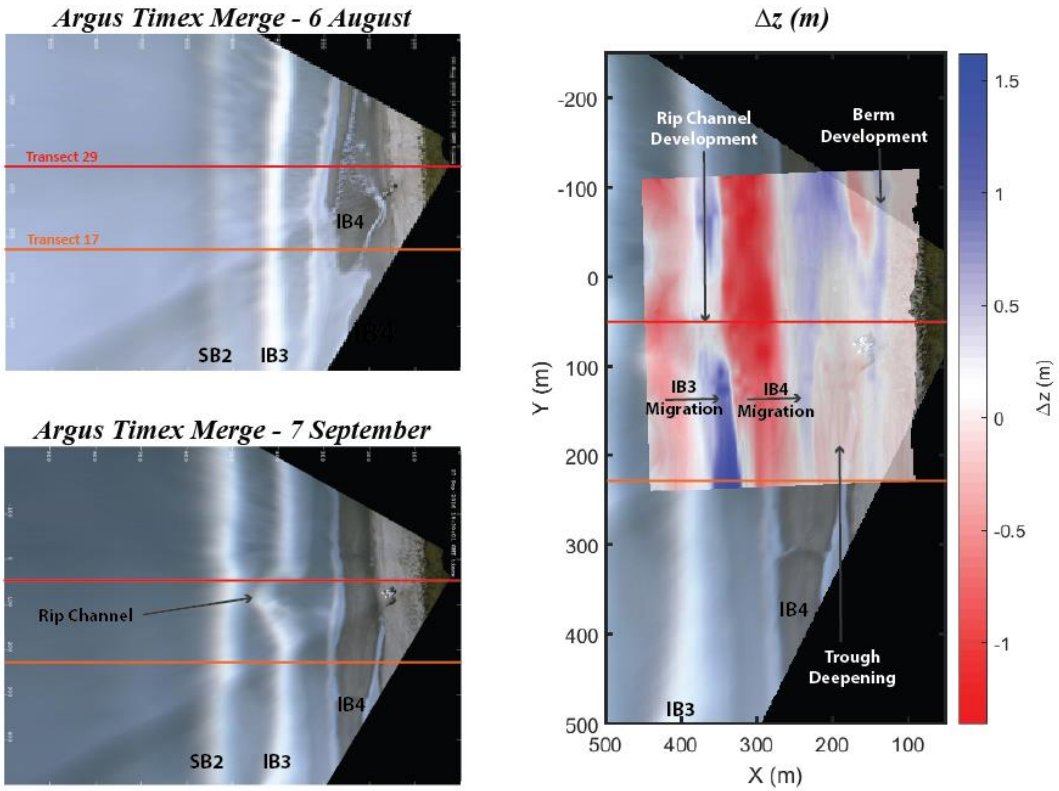

Figure 5. Argus time exposures taken at mid-tide (0.9 m NAVD88) near the start (6 August 2016, upper left panel) and end (7 September 2016, lower left panel) of the field experiment revealing changes in intertidal and nearshore morphology. Net changes in elevation in the center of study area between 2 August 2016 and 2 September 2016 are shown in the right panel.

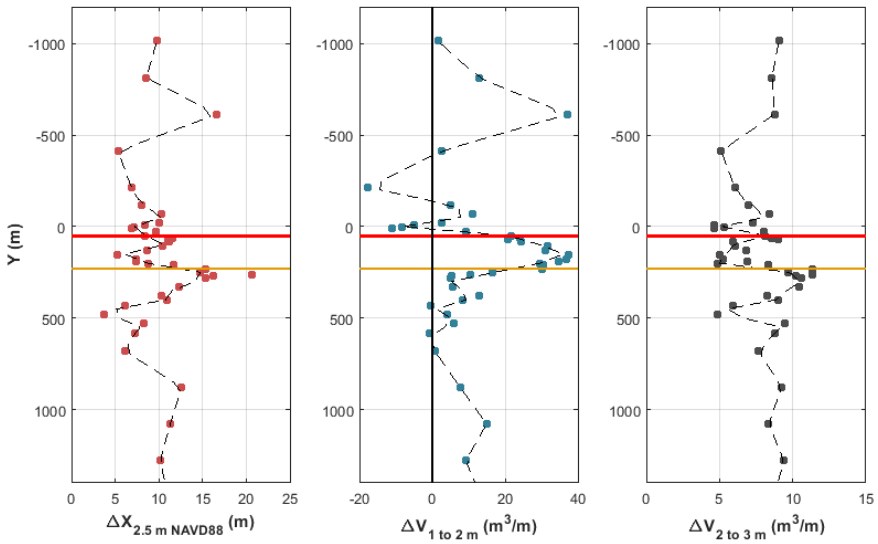

Figure 6. Alongshore variability in contour change near the berm location (left panel) and volumetric changes for specific contours in the intertidal zone (right panels) for the study site. Dotted lines show spatially averaged values.

4.2 Morphodynamic Drivers of Onshore Bar Migration

4.2.1. Temporal variability in hydrodynamics

Temporal variability in offshore waves (Figure 2), tides, and the nearshore profile (Figure 3) all influence

inner surf zone hydrodynamics. A pressure sensor continuously deployed near the base of the intertidal zone provided information on waves and water levels influencing the swash zone (Figure 7). At this location the local bed elevation decreased from 0.9 m NAVD88 to -0.2 m NAVD88 during the experiment. Associated in part with these local elevation changes, maximum wave heights at this fixed location increased during SEDEX[2]. The wave heights near the base of the intertidal zone ($H_{intertidal}$) were up to 95% of those measured offshore by the AWAC (H_o) during high tide at the beginning of September, whereas $H_{intertidal}/H_o$ rarely exceeded 50% towards the beginning of the experiment.

Wave height skewness (S) indicates that waves deviate from a purely sinusoidal form ($S = 0$) and instead are characterized by long, flat troughs in between short but high wave crests. The wave height skewness is given as:

$$S = \frac{\langle(\eta - \bar{\eta})^3\rangle}{\langle(\eta - \bar{\eta})^2\rangle^{3/2}}$$

where η is the instantaneous water surface elevation, $\bar{\eta}$ is the mean water surface elevation, the angle brackets indicates that the values are averaged over multiple waves (Brinkkemper, 2013). Skewed wave heights correspondingly result in skewed wave orbital velocities which are associated with net onshore sediment transport (e.g., Doering et al., 2001). Wave height skewness is calculated every 30 minutes when the sensor was continuously inundated as shown in Figure 7, indicating a general decrease in wave nonlinearity throughout the study period at the base of the intertidal zone. As the intertidal pressure sensor array was located at the same alongshore position of the rip channel in IB3 and because the local elevation at this location decreased by over a meter during the study period, these observed changes in $H_{intertidal}/H_o$ and S may be related to local morphologic changes. In this case, the shallow water nearshore morphology has a strong control on hydrodynamic boundary conditions to the intertidal zone.

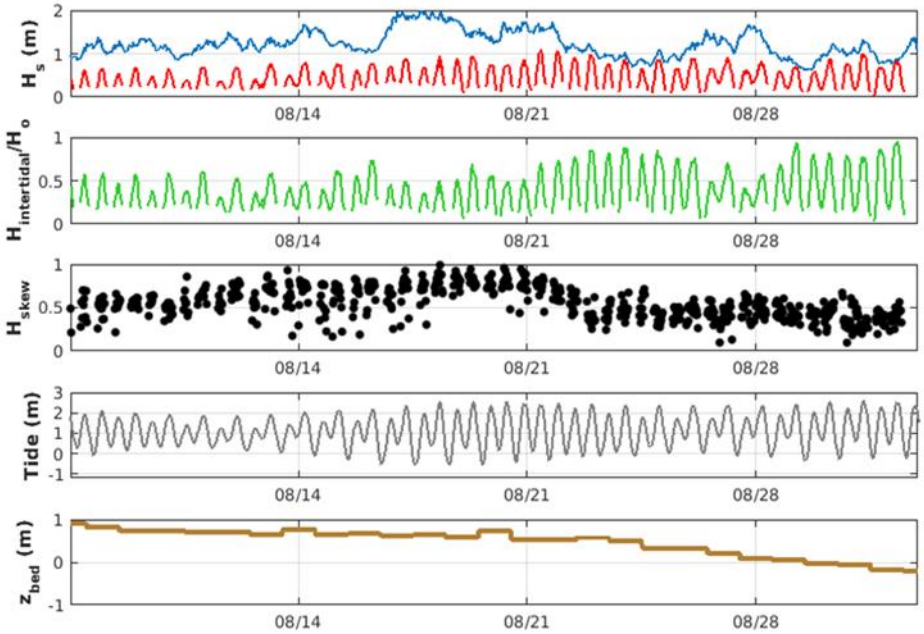

Figure 7. Temporal variability in wave height (blue = H_o, red = $H_{intertidal}$), ratio of wave heights in the intertidal zone to offshore, intertidal wave height skewness, tidal elevations (m, NAVD88), and local bed elevation (m, NAVD88) at the base of the intertidal zone

4.2.2. Spatial variability in hydrodynamics

Spatial gradients in sediment transport ultimately drive morphology change, with nonlinear wave processes generally resulting in net onshore sediment transport and corresponding onshore bar migration. Four pressure sensors in a cross-shore array continuously measured water levels during high tidal stages. The

data shows that wave heights decrease across the intertidal zone and that the waves generally become less skewed as they propagate landward (Figure 8). The least skewed waves consistently occur directly over the bar crest during high tidal stages. Based on observed morphology changes at these sensors, we infer that the combination of reduced wave energy and reduced wave nonlinearity at the bar crest at high tide may have resulted in local deposition of seaward-derived sediment near the bar crest – consistent with the observed volumetric growth of IB4 with time. At lower tidal stages individual swash events overtop the bar crest, subsequently moving sediment from the stoss slope and crest into the bar trough. This overtopping process was qualitatively observed in the field at IB3/IB4 (Figure 9).

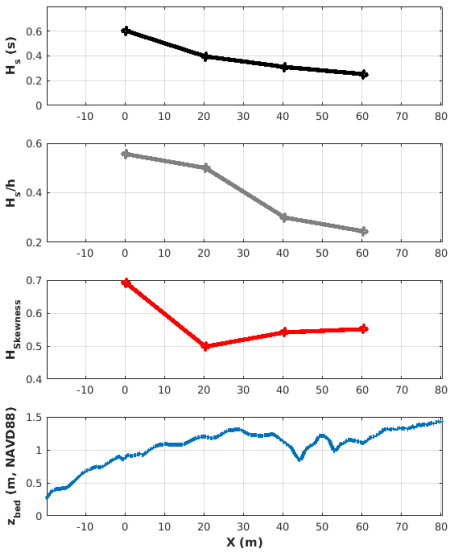

Figure 8. Representative cross-shore wave height (upper panel), wave height to local water depth ratio (upper middle panel), wave height skewness (lower middle panel) and measured bed elevations (lower panel) during high tide conditions at Transect 29

Figure 9. Overtopping of IB3 by swash

As seen in the morphology data, sediment is also transported landward from IB4 leading to the development of the berm above MHW. In the landward IB4 bar trough there is a local increase in water depths, decrease in wave heights, and increase in wave skewness (Figure 8). Decreased depth averaged return flows in the trough will reduce the local offshore directed forcing, while observed increases in wave non-linearity will promote onshore transport. The confluence of reduced offshore directed forcing and increased onshore forcing in the trough could provide a partial mechanism for continued transport landward from the IB4 bar crest leading to the development of the berm at the upper edge of the swash zone.

5. Discussion and Conclusions

A coastal field study at a dissipative beach in the U.S. Pacific Northwest tracked the evolution of nearshore and beach morphology in summer 2016. Two intertidal sandbars moved onshore at rates of up to 12 m/day, but with average daily rates typically between 1 and 3 m. As the most landward intertidal bar reached the mean high water contour near the end of the study, sediment shed off from this bar contributed to the development of a berm at the upper limit of wave runup. Onshore intertidal sandbar migration occurred across the entire 2.5 km study site, although alongshore variability in intertidal volume changes and berm growth were noted. Some of this alongshore variability can be attributed to specific morphologic features. For example, a rip channel resulted in increased wave energy within the adjacent intertidal zone. In response, the intertidal bar landward of the channel reduced in height - highlighting the complex morphodynamic feedback mechanisms driving intertidal sandbar migration.

In order to explore the processes driving the observed bar behavior, a series of hydrodynamic measurements were made in the intertidal zone. Preliminary results suggest that cross-shore gradients in nonlinear wave properties and temporal variability in the amount of wave energy within the intertidal zone are likely important for influencing intertidal sandbar dynamics.

Acknowledgements

This study was funded by the U.S. National Science Foundation under grant EAR-1561847. Thanks to George Kaminsky (Washington Department of Ecology), Guy Gelfenbaum (United States Geological Survey), Jack Puleo (University of Delaware), and Eugene Bodrero (Dyacon, Inc.) for lending equipment for SEDEX^2. Many researchers were involved in field data collection during the study – we sincerely thank them for their contributions to these efforts.

References

Aagaard, T., Hughes, M., Baldock, T., Greenwood, B., Kroon, A., and Power, H., 2012. Sediment transport processes and morphodynamics on a reflective beach under storm and non-storm conditions. *Marine Geology*, 326-328, 154–165.

Allan, J. C., and Komar, P. D., 2002. Wave climate change and coastal erosion in the US Pacific Northwest. *Ocean Wave Measurement and Analysis*, 680-689.

Barnard, P., Hoover, D., Hubbard, D., Snyder, A., Ludka, B., Allan, J., Kaminsky, G., Ruggiero, P., Gallien, T., Gabel, L., Cohn, N., Anderson, D., and Serafin, K., 2017. Extreme oceanographic forcing and coastal response due to the 2015-2016 El Niño. *Nature Communications*, 8.

Brinkkemper, J. A., 2013. Modeling the cross-shore evolution of asymmetry and skewness of surface gravity waves propagating over a natural intertidal sandbar. Master's thesis. Utrecht University.

Cohn, N., Anderson, D., and Ruggiero, P., 2015. Observations of intertidal bar welding along a high energy, dissipative coastline. *Proceedings of the Coastal Sediments Conference*. San Diego, CA.

Di Leonardo, D., and Ruggiero, P., 2015. Regional scale sandbar variability: Observations from the US Pacific Northwest. *Continental Shelf Research*, *95*, 74-88.

de Vries, S., Arens, S. M., de Schipper, M. A., and Ranasinghe, R. 2014. Aeolian sediment transport on a beach with a varying sediment supply. *Aeolian Research*, *15*, 235-244.

de Vries, S., Verheijen, A., Hoonhout, B., Vos, S., Cohn, N., and Ruggiero, P. (this issue) Measured spatial variability of beach erosion due to aeolian processes. *Proceedings of the Coastal Dynamics Conference 2017*. Hensingor, Denmark.

Doering, J. C., Elfrink, B., Hanes, D. M., and Ruessink, G., 2001. Parameterization of velocity skewness under waves and its effect on cross-shore sediment transport. *Proceedings of the Coastal Engineering Conference 2000*, 1383-1397.

Elgar, S., Gallagher, E.L., and Guza, R.T., 2001. Nearshore sandbar migration. *Journal of Geophysical Research: Oceans*, 106 (C6): 11623-11627.

Holman, R. A., and Stanley, J., 2007. The history and technical capabilities of Argus. *Coastal Engineering*, 54(6), 477-491.

Houser, C., 2009. Synchronization of transport and supply in beach-dune interaction. *Progress in Physical Geography*, 33 (6): 733-746.

Kroon, A., and Masselink, G. (2002). Morphodynamics of intertidal bar morphology on a macrotidal beach under low-energy wave conditions, North Lincolnshire, England. *Marine Geology*, 190(3), 591-608.

Masselink, G., Kroon, A., and Davidson-Arnott, R. G. D., 2006. Morphodynamics of intertidal bars in wave-dominated coastal settings—a review. *Geomorphology*, 73(1), 33-49.Ruggiero, P., Kaminsky, G. M., Gelfenbaum, G., and Cohn, N., 2016. Morphodynamics of prograding beaches: A synthesis of seasonal-to century-scale observations of the Columbia River littoral cell. *Marine Geology*, 376: 51-68.

Ruggiero, P., Kaminsky, G. M., Gelfenbaum, G., and Cohn, N., 2016. Morphodynamics of prograding beaches: A synthesis of seasonal-to century-scale observations of the Columbia River littoral cell. *Marine Geology*, *376*, 51-68.

Ruggiero, P., Kaminsky, G.M., Gelfenbaum, G., and Voigt, B., 2005. Seasonal to interannual morphodynamics along a high-energy dissipative littoral cell. *Journal of Coastal Research*, 21(3): 553-578.

Sunamura, T., and Takeda, I., 1984. Landward migration of inner bars. *Marine Geology*. 60 (1-4), 63-78.

Thornton, E. B., Humiston, R. T., and Birkemeier, W., 1996. Bar/trough generation on a natural beach. *Journal of Geophysical Research: Oceans*, 101(C5): 12097-12110.

Wijnberg, K. and Kroon, A., 2002. Barred beaches. *Geomorphology*, 48: 103-110.